

Hybrid Displacement Models for a Physically Nonlinear Analysis of Three-dimensional Concrete Structures

João Miguel de Oliveira Durães Alves Martins

Abstract: The main purpose of this communication is to present and discuss a hybrid displacement model for a physically nonlinear analysis of three-dimensional plain concrete structures using isotropic continuum nonlocal damage models. Although this formulation leads to a large number of degrees of freedom, a high level of sparsity is achieved for the global stiffness matrix in elastic regime using complete series of orthonormal Legendre polynomials as approximation functions. Furthermore, analytical expressions are known for integrals involving these functions, which makes computation even more efficient while the stiffness matrix is computed based on physical linearity. The efficiency of the model when damage is introduced is essential to assess the competitiveness of this formulation, since sparsity decreases considerably. In this context, two distinct three-dimensional physically nonlinear analyses are implemented using two different damage models so that a comprehensive set of tests can be performed. The results make it clear that these models, though effective, have high computational costs.

Key words: Finite Elements, Hybrid Displacement Model, Continuum Damage Mechanics, Three-dimensional Concrete Structures, Legendre Polynomials

1. Introduction

Most engineering problems can be expressed mathematically in terms of differential equations, with or without known analytical solution. The search for a numerical systematic way of solving these problems led to finite element methods, derived from the displacement method, well-known and theoretically established in the structural analysis framework. They have been broadly used to solve continuous mechanics problems applied to structures with irregular geometries, complicated boundary conditions and non-homogeneous material properties (Zienkiewicz, 1977). However, the conventional formulations use conforming displacement elements, which, despite their intuitiveness, also introduce some limitations. On the one hand, the solutions thus obtained overvalue the ultimate load of the structure according to the kinematic theorem of plastic analysis. On the other hand, according to (Zienkiewicz, 1977), this regular formulation is not fit for problems with singularities, such as cracks or sharp wedges, because convergence rates can not improve effectively even with highly accurate regular elements with high-order polynomial interpolation functions

For over a decade, non-conventional formulations for the finite element method have been developed by the Structural Analysis Research Group of Instituto Superior Técnico in order to stand as attractive alternatives to the regular formulation. This work focuses on one of these formulations, presented by (Freitas et al, 1999), named hybrid because two fields are approximated, one in the domain of the element and other on its boundary, and called a displacement model due to the fact that inter-element continuity is implemented enforcing on average the compatibility conditions. Hence, the approximations used are the displacement field in the domain of each finite element and the field of applied stresses on the kinematic boundary, which includes inter-element boundaries. Meshing is not as complicated as it is in conventional formulations since accurate solutions are generally obtained using macro-elements meshes combined with effective p-refinement procedures.

(Silva, 2006) shows that it is possible to model realistically concrete's behaviour by including damage in these formulations. In fact, cracks in concrete structures are common because of the poor resistance of the material to tensile stresses, making it inaccurate to disregard damage and its consequences in the presence of relevant positive strains. Therefore, the hybrid displacement models presented in this work consider nonlinear behaviour of concrete associated with cracking. The advantages that come from these procedures concern the possibility to determine the maximum resistance and to analyse post-peak behaviour of a concrete structure and, thus, explore its ductility and achieve a more economical design. According to (Lopes et al, 2008), this is extremely important in earthquake design. In fact, the specificity of the seismic load, which has relatively high return periods and acts as a prescribed displacement, makes it not only possible but also ingenious to explore the post-peak behaviour of any structure.

Having this starting point, the purpose of this work is to develop a three-dimensional hybrid displacement model concerning continuum damage without making it inefficient, but reproducing the nonlinear behaviour of concrete considering softening of the material. Among various possible

models, two scalar isotropic continuum damage models following the same kind of regularization techniques are chosen due to the simplicity of their implementation, Comi and Perego's damage model (Comi and Perego, 2001) and Mazars damage model (Mazars, 1984).

The greatest handicap of these models is the generation of an unwieldy number of generalized degrees of freedom. Whereas in elastic regime the well-known properties of the used approximation functions, orthonormal Legendre polynomials, make these approaches competitive if thoroughly optimized, one of the objectives of this work is to assess the efficiency when damage is introduced, since part of this optimization process is no longer possible and numerical integration is unavoidable. In fact, analytical expressions involving the integrals that need to be computed are used whenever possible to achieve a better performance of the models, representing a new approach, since the analytical expression for the integration of the product of two derivatives of Legendre polynomials had not yet been published by the time this work was being developed and were therefore deduced.

Some assumptions had to be made during the course of the work, in order to simplify the problem, focusing on what is important and without compromising the proposed objectives. First of all, the hypothesis of geometrical linearity is supposed to remain valid. Temperature is not an intervenient factor; hence energy dissipation has origin only in mechanical phenomena. The undamaged material is considered homogeneous. The damage models are isotropic. The constitutive model may be considered elastic in the sense that permanent strains are not considered, but just a degradation of the elastic properties, which allows the use of a secant law for the stiffness relation always regarding the origin of a stress-strain coordinate system. Since the implemented model assumes monotonic loading, provided the material parameters are carefully calibrated, the stress responses are qualitatively the same as in plasticity models (Borino and De Borst, 2000).

2. Problem formulation

While the laws of equilibrium and compatibility come from general three-dimensional mechanics, the material of which the structure is made as well as its geometry and load case determine the most appropriate constitutive relation to use. Experiments show that the constitutive behaviour of plain concrete is clearly nonlinear and quasibrittle. According to (Bascoul, 1996), when a concrete structure is loaded, microcracks occur at elemental level at the weakest points, which are located around the interfacial zone between the cement paste and the aggregates. These distributed microcracks tend to group and form continuous cracks as load increases. This process explains both the nonlinear behaviour of concrete pre-peak and the softening effect post-peak. However, it is computationally unwieldy to explicitly consider all these factors in the nonlinear formulation of the problem, in which the material is, for the sake of simplicity and model efficiency, supposed to be homogeneous. The proposal of Continuum Damage Mechanics is to abridge the resulting permanent loss of stiffness and resistance in a single variable, damage, that subliminally evaluates the creation

and growth of microvoids or microcracks, discontinuities in a medium considered as continuous at a larger scale (Lemaitre and Desmorat, 2005).

In this formulation, the framework presented by (Zienkiewicz, 1977) is applied to a three dimensional generic solid considered in a Cartesian coordinate system (x, y, z) . Its domain is represented by V (volume), while the boundary Γ can be divided into Γ_u , kinematic boundary, also known as Dirichlet boundary, i.e. where displacements u are prescribed, and Γ_σ , static boundary, stress boundary or Neumann boundary, i.e. where stresses are known. When displaying the mathematical relations in matrix form, the applied external loads in V are represented by \mathbf{b} , whereas \mathbf{t}_γ stands for the ones applied on Γ_σ . It is assumed that \mathbf{t}_γ is composed only of distributed forces over surfaces.

2.1. Equilibrium conditions

Since the stress tensor is symmetric, it is simply represented by $\boldsymbol{\sigma}$, the stresses vector. Considering that \mathbf{D} is the equilibrium differential operator for three-dimensional elasticity and \mathbf{N} is the matrix of the components of the unit outward normal vector associated with the differential operator \mathbf{D} . Then, the equilibrium conditions come as follows:

$$\mathbf{D} \boldsymbol{\sigma} + \mathbf{b} = 0 \quad \text{in } V, \quad (1)$$

$$\mathbf{N} \boldsymbol{\sigma} = \mathbf{t}_\gamma \quad \text{on } \Gamma_\sigma. \quad (2)$$

2.2. Compatibility conditions

Considering \mathbf{D}^* as the compatibility differential operator and $\boldsymbol{\varepsilon}$ as the strains vector, taking advantage from the symmetry of the strains tensor, the compatibility conditions are:

$$\mathbf{D}^* \mathbf{u} = \boldsymbol{\varepsilon} \quad \text{in } V, \quad (3)$$

$$\mathbf{u} = \bar{\mathbf{u}} \quad \text{on } \Gamma_u. \quad (4)$$

Since the assumption of geometric linearity is supposed to be valid, \mathbf{D} and \mathbf{D}^* are adjoint differential operators, thus, considering n as the order of the derivative of \mathbf{D}_{ji} :

$$\mathbf{D}^*_{ij} = (-1)^{n+1} \mathbf{D}_{ji}. \quad (5)$$

2.3. Constitutive relationship

The constitutive relationship is nonlinear and the tensor which materializes this relation is designated by $\tilde{\mathbf{K}}$. This is a fourth-order tensor relating two second-order tensors, $\boldsymbol{\sigma}$ and $\boldsymbol{\varepsilon}$:

$$\boldsymbol{\sigma} = \tilde{\mathbf{K}} : \boldsymbol{\varepsilon}. \quad (6)$$

Considering d as the scalar damage variable

$$\tilde{\mathbf{K}} = (1 - d) \mathbf{K}, \quad (7)$$

where \mathbf{K} represents the stiffness tensor in elastic regime and depends on the elastic parameters E and ν , the Young's modulus and the Poisson's ratio, respectively. Following equation (7), the behaviour of concrete may be considered elastic while the variable damage is null, i.e., while strains are smaller than those that cause crack initiation and have never before been higher.

3. Damage models

A complete approach to damage mechanics is presented in (Lemaitre and Desmorat, 2005), where the three steps of modelling different materials' behaviour is explained according to the thermodynamics of irreversible processes. Summarizing briefly in order to introduce the applied damage models, these three steps are:

1. Definition of state variables, which might be observable or internal and are used to characterize the state of the mechanism. The choice of the state variables depends on the physical mechanisms of damage;
2. Definition of a state potential, such as the Helmholtz specific free energy (ψ) used in Continuum Damage Mechanics, and of the variables associated with the internal state variables. In this step, the laws of thermoelasticity are derived;
3. Definition of a dissipation potential, f . The kinetic laws governing the evolution of the state variables associated with the dissipative mechanisms are derived in this step.

(Lemaitre and Desmorat, 2005) alluded that the definitions applied at each step must meet the experimental results and purpose of use, yielding various damage models. For instance, considering the dissipation potential written in terms of two system variables, generically called a and k :

$$f(a,k) = a - k, \text{ with } k(t) = \max \{ \max_{\tau \leq t} [a(\tau)], k_0 \} \quad (8)$$

where t stands for time, and k is equal to a threshold value k_0 until this limit is overcome by a ; from there on, it takes the maximum value reached by a .

Furthermore, when modelling a material with no viscosity under static or quasi-static loading, time is not relevant. Based on this premise, the complete loading or unloading conditions, also known as Kuhn-Tucker conditions, might be derived, yielding:

$$f \leq 0, \quad \dot{k} \geq 0, \quad f \dot{k} = 0. \quad (9)$$

3.1. Comi and Perego's damage model

(Comi and Perego, 2001) propose an isotropic damage model dependent on one scalar variable alone, d , which stands as an internal state variable. Another internal state variable, ξ , is introduced in equation (10) to define the Helmholtz specific free energy (ψ) and has kinematic nature. The strains ($\boldsymbol{\epsilon}$) play the role of observable state variables. The associated variables are the stress vector $\boldsymbol{\sigma}$

(equation (11)), the elastic energy release rate Y (equation (12)) and the thermodynamic force χ (equation (13)). These variables are defined as the derivatives of ψ with respect to each state variable:

$$\psi = \frac{1}{2} (1 - d) \boldsymbol{\varepsilon} : \mathbf{K} : \boldsymbol{\varepsilon} + \psi_{in}(\xi); \quad (10)$$

$$\boldsymbol{\sigma} = \frac{\partial \psi}{\partial \boldsymbol{\varepsilon}} = (1 - d) \mathbf{K} : \boldsymbol{\varepsilon}, \quad (11)$$

$$Y = -\frac{\partial \psi}{\partial d} = \frac{1}{2} \boldsymbol{\varepsilon} : \mathbf{K} : \boldsymbol{\varepsilon}, \quad (12)$$

$$\chi = \frac{\partial \psi}{\partial \xi} = \psi'_{in}(\xi). \quad (13)$$

In equation (10), $\psi_{in}(\xi)$ expresses the inelastic energy density, so that microstructural rearrangements due to damage evolution are taken into account.

The dissipation potential is written in terms of Y and χ , according to the following equation:

$$f(Y - \chi) = Y - \chi = \frac{1}{2} \boldsymbol{\varepsilon} : \mathbf{K} : \boldsymbol{\varepsilon} - \chi \leq 0 \quad (14)$$

The evolution of the internal variables is defined in terms of the derivatives of the dissipation potential with respect to the associated variables. Hence:

$$\dot{d} = \frac{\partial f}{\partial Y} \dot{Y} = \dot{\gamma}, \quad \dot{\xi} = -\frac{\partial f}{\partial \chi} \dot{\chi} = \dot{\gamma}, \quad (15)$$

in which γ is a positive scalar. As a consequence of the above equations, the damage variable d takes the same value of the internal variable ξ and of the positive scalar γ , defining that they are all null before damage is initiated.

Moreover, (Comi and Perego, 2001) deduce the following expression for the thermodynamic force:

$$\chi = \frac{\partial \psi}{\partial \xi} = k \ln^n \left(\frac{c}{1 - \xi} \right), \quad (16)$$

which requires the calibration of the material parameters k , n and c to model the behaviour of the material. Taking this equation, assuming ξ to be equal to d and bearing in mind that damage evolves when equation (14) corresponds to an equality, Comi and Perego's evolution of damage law yields:

$$d = 1 - \frac{c}{\exp \left[\sqrt[n]{\frac{Y}{k}} \right]}. \quad (17)$$

The damage initiation threshold of this model is $Y = k \ln^n(c)$. For Y greater than this, the behaviour of the material is nonlinear.

The original version of this model does not differentiate between the behaviour of the material under compression or tension, which is not realistic. Therefore, an additional condition is imposed so that damage only exists if the trace of the strains tensor is greater than zero. This quantity is independent of the coordinate system and is called the volumetric strain. Imposing that it has to be

greater than zero is the same as restricting the evolution of damage to points of the structure where elongation occurs. Consequently, this model is mainly adequate to structures essentially under tensile stresses.

3.2. Mazars damage model

As introduced by (Mazars, 1984), Mazars damage models uses one scalar damage variable, called d , that depends only on the tensile strains of the material. The latter are observable state variables and the former is an internal state variable. In order to consider only the tensile extensions, the mathematical formulation uses the Macaulay brackets, $\langle (\cdot) \rangle_+$, which return the value of the argument if it is positive, and zero otherwise. It is also possible to return the value of the argument if it is negative, and zero otherwise, which is also introduced with pointed brackets, $\langle (\cdot) \rangle_-$.

In a three-dimensional space the strain is a tensor field, meaning the magnitude of the strain in a certain point of the structure depends not only on the localization of the point but also on a direction of analysis. Therefore, according to Mazars model an equivalent strain $\tilde{\epsilon}$ is used, which attempts to summon the tensor field to a single observable state variable, $\tilde{\epsilon} = \tilde{\epsilon}(\epsilon)$. This value aims to define the accumulated tensile strain in the material, as stated in (Mazars et al, 1991) and, hence, assembles the positive principal strains in the following way:

$$\tilde{\epsilon} = \sqrt{\langle \epsilon_I \rangle_+^2 + \langle \epsilon_{II} \rangle_+^2 + \langle \epsilon_{III} \rangle_+^2} = \sqrt{\sum_{i=I}^{III} \langle \epsilon_i \rangle_+^2}. \quad (18)$$

Since these assumptions must be applicable to more complex strain fields than just uniaxial loading, the dissipation potential of Mazars damage model is a function of the equivalent strain:

$$f(\tilde{\epsilon}, d) = \tilde{\epsilon} - \chi(d) \leq 0, \text{ where } \chi(0) = \epsilon_{d0} \text{ and } \chi(d(t)) = \max \{ \max_{\tau \leq t} [\tilde{\epsilon}(\tau)], \epsilon_{d0} \} \quad (19)$$

The kinetic laws governing the evolution of damage yield:

$$\dot{d} = 0 \text{ if } f < 0 \text{ or } f = 0 \text{ and } \dot{f} < 0; \quad (20)$$

$$\dot{d} = F(\tilde{\epsilon}) \langle \dot{\tilde{\epsilon}} \rangle_+ \text{ if } f = 0 \text{ and } \dot{f} = 0. \quad (21)$$

$F(\tilde{\epsilon})$ is a continuous and positive function of the equivalent strain such that damage increases whenever the equivalent strain increases. This function is different whether its purpose is to model a uniaxial compression or tension state, which results in the definition of two independent scalar variables, d_c and d_t respectively, given by:

$$\dot{d}_t = F_t(\tilde{\epsilon}) \langle \dot{\tilde{\epsilon}} \rangle_+, \quad (22)$$

$$\dot{d}_c = F_c(\tilde{\epsilon}) \langle \dot{\tilde{\epsilon}} \rangle_+, \quad (23)$$

where,

$$F_t(\tilde{\epsilon}) = \frac{\epsilon_{d0} (1 - A_t)}{\tilde{\epsilon}^2} + \frac{A_t B_t}{\exp[B_t (\tilde{\epsilon} - \epsilon_{d0})]}, \quad (24)$$

$$F_c(\tilde{\epsilon}) = \frac{\epsilon_{d0} (1 - A_c)}{\tilde{\epsilon}^2} + \frac{A_c B_c}{\exp[B_c (\tilde{\epsilon} - \epsilon_{d0})]} . \quad (25)$$

The integration of expressions (22) and (23) yields:

$$d_t(\tilde{\epsilon}) = 1 - \frac{\epsilon_{d0} (1 - A_t)}{\tilde{\epsilon}} - \frac{A_t}{\exp[B_t (\tilde{\epsilon} - \epsilon_{d0})]} , \quad (26)$$

$$d_c(\tilde{\epsilon}) = 1 - \frac{\epsilon_{d0} (1 - A_c)}{\tilde{\epsilon}} - \frac{A_c}{\exp[B_c (\tilde{\epsilon} - \epsilon_{d0})]} . \quad (27)$$

These expressions are only applicable if the equivalent strain is greater than the initial damage threshold; elsewhere damage is equal to zero. Furthermore, parameters A_t and B_t (related to tension) and A_c and B_c (related to compression) are, just like ϵ_{d0} , calibrated based on experiments on cylinders, the first-named under uniaxial tension with controlled deformations and the last-named under uniaxial compression with controlled displacements (Mazars et al, 1991).

One of the advantages of this damage model is that these relatively simple assumptions and expressions can be generalised to more complex states of stress, retaining the concept of only one damage variable d , which is obtained by linear combination of (26) and (27):

$$d = \alpha_t d_t + \alpha_c d_c , \quad (28)$$

constraining α_t and α_c to observe $\alpha_t + \alpha_c = 1$. These parameters α_t and α_c are determined according to the work of (Perego, 1990):

$$\alpha_t = \frac{\sum_{i=1}^{\text{III}} \langle \epsilon_{Ti} \rangle_+}{\sum_{i=1}^{\text{III}} \langle \epsilon_{Ti} \rangle_+ + \sum_{i=1}^{\text{III}} \langle \epsilon_{Ci} \rangle_+} \quad \text{and} \quad \alpha_c = \frac{\sum_{i=1}^{\text{III}} \langle \epsilon_{Ci} \rangle_+}{\sum_{i=1}^{\text{III}} \langle \epsilon_{Ti} \rangle_+ + \sum_{i=1}^{\text{III}} \langle \epsilon_{Ci} \rangle_+} , \quad (29)$$

where

$$\epsilon_{Ti} = \frac{1+\nu}{E} \langle \tilde{\sigma}_i \rangle_+ - \frac{\nu}{E} \sum_{j=1}^{\text{III}} \langle \tilde{\sigma}_j \rangle_+ \mathbf{I} \quad \text{and} \quad \epsilon_{Ci} = \frac{1+\nu}{E} \langle \tilde{\sigma}_i \rangle_- - \frac{\nu}{E} \sum_{j=1}^{\text{III}} \langle \tilde{\sigma}_j \rangle_- \mathbf{I} . \quad (30)$$

In the previous expressions, \mathbf{I} is the identity tensor and $\tilde{\sigma}_i/\tilde{\sigma}_j$ are the principal effective stresses.

3.3. Strain localization and regularization methods

Mazars damage model takes damage directly as a function of the strain field, while in Comi and Perego's model damage is computed considering the elastic energy release rate, which, nevertheless, is a function of the strain field. Since the strain field varies from one point of the structure to another, damage itself is a space-dependent variable. However, the result thus obtained without further refinement is not reliable once it leads to an unrealistic concentration of high magnitude strains. Besides, damage concentrates in an element which is smaller if the mesh is refined, up to a point when failure occurs in a layer of infinitesimal thickness and without dissipation of energy, according to (Bažant, 1984) and (Mazars et al, 1991). However, this strain localization is not the only problem as there is also a phenomenon of loss of ellipticity presented by (Lemaitre et al, 2002),

which is related to the ill-posedness of the boundary value problems, leading to an infinite number of linearly independent solutions that might not depend continuously on the data. On the whole, a local change of the type of the boundary value problem during a loading process in a physically nonlinear analysis from elliptic to hyperbolic may happen. The same authors give the example of the appearance of discontinuity surfaces in softening materials.

In this communication, a regularization method based on nonlocal continuum damage solves these problems. Nonlocal behaviour assumes that there is a spatial weighting of a variable related to the strain softening process (Bažant and Pijaudier-Cabot, 1988). In this work, the mathematical implementation of the nonlocal integral averaging model is achieved by applying a spatial weighting to the elastic energy release rate, Y , in Comi and Perego's model (Comi et al, 2002) and to the equivalent strain, $\tilde{\epsilon}$, in Mazars model (Mazars et al, 1991), using the normalized Gaussian weight function:

$$W(x,s) = \frac{1}{W_0(x)} \exp \left[-\frac{\|x-s\|^2}{2 l^2} \right] \quad (31)$$

with

$$W_0(x) = \int_V \exp \left[-\frac{\|x-s\|^2}{2 l^2} \right] dV, \quad (32)$$

considering x is the location where the quantity is evaluated, s is the general coordinate vector, V is the volume of the body and $W(x,s)$ is the weighting function. Parameter l corresponds to the characteristic length and adjusts the weight of the analysed neighbourhood centered at each evaluation point (Mazars et al, 1991).

4. Mathematical description of the hybrid displacement model

Hybrid displacement models are characterized by independent approximations of the displacement field in the domain of each finite element \mathbf{u} and the field of applied stresses along the kinematic boundary, including inter-element boundaries, \mathbf{t}_γ . These approximations can be written as follows:

$$\mathbf{u} = \mathbf{U}_v \mathbf{q} \quad \text{in } V, \quad (33)$$

$$\mathbf{t}_\gamma = \mathbf{T} \mathbf{p} \quad \text{on } \Gamma_u. \quad (34)$$

The approximation functions for the displacements in the domain are listed in the matrix \mathbf{U}_v and the matrix \mathbf{T} stores the approximation functions for the stresses along the kinematic boundary of each element. This formulation allows them to be independent from each other and to have different values in each direction of the coordinate system. Vectors \mathbf{q} and \mathbf{p} gather the weights associated to each approximation, displacements in the domain and stresses on the kinematic boundary,

respectively. In conventional formulations, the approximation functions are enforced so that these vectors represent nodal quantities. In this hybrid formulation, they are generalised displacements in the domain in the case of \mathbf{q} and generalised stresses on the kinematic boundary in the case of \mathbf{p} .

The generalised forces in the domain \mathbf{Q}_V and the generalised displacement along the kinematic boundary \mathbf{v} may be defined by imposing that the dual quantities in the continuous and discrete models perform the same work (Freitas et al, 1999). Therefore:

$$\mathbf{Q}_V = \int \mathbf{U}_V^T \mathbf{b} \, dV, \quad (35)$$

$$\mathbf{v} = \int \mathbf{T}^T \bar{\mathbf{u}} \, d\Gamma_u. \quad (36)$$

The equilibrium in the domain is enforced on average, resulting in the weak formulation of the balance laws:

$$\int \mathbf{U}_V^T (\mathbf{D} \boldsymbol{\sigma} - \mathbf{b}) \, dV = 0. \quad (37)$$

Similarly, when the same reasoning is applied to the compatibility along the kinematic boundary, the following expression is deduced:

$$\int \mathbf{T}^T (\mathbf{u} - \bar{\mathbf{u}}) \, d\Gamma_u = 0. \quad (38)$$

The following expression results from the integration by parts of (37) taking (35) into account:

$$-\int (\mathbf{D}^* \mathbf{U}_V)^T \boldsymbol{\sigma} \, dV + \int (\mathbf{N}^* \mathbf{U}_V)^T \boldsymbol{\sigma} \, d\Gamma_u + \int (\mathbf{N}^* \mathbf{U}_V)^T \boldsymbol{\sigma} \, d\Gamma_\sigma = -\mathbf{Q}_V. \quad (39)$$

It is then possible to write an equilibrium equation by working the previous expression, considering the assumed constitutive relation, the derived compatibility equation in the domain and the equilibrium relation on the boundary, as well as the approximations established in (33) and (34):

$$\tilde{\mathbb{K}} \mathbf{q} - \mathbf{B} \mathbf{p} = \mathbf{Q}_V + \mathbf{Q}_\Gamma \text{ in } V, \quad (40)$$

considering:

$$\tilde{\mathbb{K}} = \int (\mathbf{D}^* \mathbf{U}_V)^T \tilde{\mathbb{K}} (\mathbf{D}^* \mathbf{U}_V) \, dV \quad (41)$$

$$\mathbf{B} = \int (\mathbf{U}_V)^T \mathbf{T} \, d\Gamma_u \quad (42)$$

$$\mathbf{Q}_\Gamma = \int (\mathbf{U}_V)^T \mathbf{t}_\gamma \, d\Gamma_\sigma \quad (43)$$

The compatibility equation along the kinematic boundary is also necessary to solve the problem and emerges from including the approximations defined in (33) in (38):

$$-\mathbf{B}^T \mathbf{q} = -\mathbf{v} \text{ on } \Gamma_u. \quad (44)$$

Combining (40) and (44), the governing system to solve a problem using a hybrid displacement model is symmetric and given by:

$$\begin{bmatrix} \tilde{\mathbb{K}} & -\mathbf{B} \\ -\mathbf{B}^T & 0 \end{bmatrix} \begin{Bmatrix} \mathbf{q} \\ \mathbf{p} \end{Bmatrix} = \begin{Bmatrix} \mathbf{Q}_V + \mathbf{Q}_\Gamma \\ -\mathbf{v} \end{Bmatrix} \quad (45)$$

It is worth noticing that the operator \mathbf{B}^T alone is responsible for binding elements and is therefore called the compatibility operator.

5. Implementation

A proper choice of approximation functions is essential to the efficiency of the model. Thus, their properties must be explored and the choice of the maximum degrees of approximation should minimize the appearance of spurious modes. In general, the degree of approximation of the displacements is taken as the degree of approximation of the stresses plus one, since, according to the constitutive equation, the maximum degree of the stresses approximation is equal to the one of the strains and the strains are the result of the derivative of the displacements.

Orthonormal Legendre polynomials defined in a local domain corresponding to a parent hexahedron ($\xi, \eta, \zeta \in [-1.0, 1.0]$) are used in the developed models. Diverse analytical expressions involving Legendre polynomial are presented by (Pereira and Freitas, 2000). However, the analytical expression for the integration of the product of two derivatives of Legendre polynomials had not been published by the time these studies were developed and so it was deduced by the author with the following conclusion:

$$\int_{-1}^1 L'_i L'_j dx = \begin{cases} \alpha_{ij} \sqrt{(2i+1)(2j+1)}, & \text{if } i + j \text{ even} \\ 0, & \text{otherwise} \end{cases} \quad (46)$$

where,

$$\alpha_{ij} = \begin{cases} \frac{i+1}{2} \times i, & \text{if } i < j \\ \frac{j+1}{2} \times j, & \text{otherwise} \end{cases} \quad (47)$$

and L_n represents an orthonormal Legendre polynomial of the n^{th} degree

Using these polynomials, it is possible to integrate faster and more accurately using analytical expressions instead of numerical quadrature. Besides, these polynomials assure a numerical stability that distinguishes them from other sets of polynomials and introduce a level of sparsity in the governing system in elastic regime, which compensates for the high number of generated degrees of freedom. However, this does not stand when the structural operators are nonlinear, since the entrances of the elementary stiffness matrix result of the integral of the product of Legendre polynomials with damage, which also varies in the domain. The inevitable numerical integration is implemented in this work with Lobatto points, which include points located on the boundary of the considered interval, unlike Gauss quadrature (Beyer, 1987).

An adequate process of solving the nonlinear governing system that comes from considering damage is to implement an incremental and iterative process. Damage is, hence, considered incrementally as the result of load applied in successive load steps, being each step solved by an iterative process due to the nonlinear relation between loads and strains. The secant method is applied in the present work. After each iteration, the process reaches a different value for the deformation, which means that the value of damage has to be recomputed considering a regularization method.

6. Validation

The validation of the model is performed comparing the results obtained with both damage models in the analysis of an L-shaped structure. Furthermore, Comi and Perego's damage model is applied in the study of a fixed-fixed beam, a classic of strength of materials. In these examples, $E = 29200$ MPa and $\nu = 0.20$, Comi and Perego's material parameters are $k = 5.8 \times 10^{-14}$ MPa, $n = 12$ and $c = 405$ and Mazars' material parameters are $A_t = 0.30$, $B_t = 8000$, $A_c = 0.85$, $B_c = 1050$ and $\epsilon_{d0} = 9.34 \times 10^{-5}$.

6.1. Analysis of an L-shaped structure

Figure 1 depicts an L-shaped structure with full moment connection on the basis and a uniform imposed displacement at the L's tip, \bar{u} . The structure was modelled taking $n_v = 6$ and $n_g = 5$.

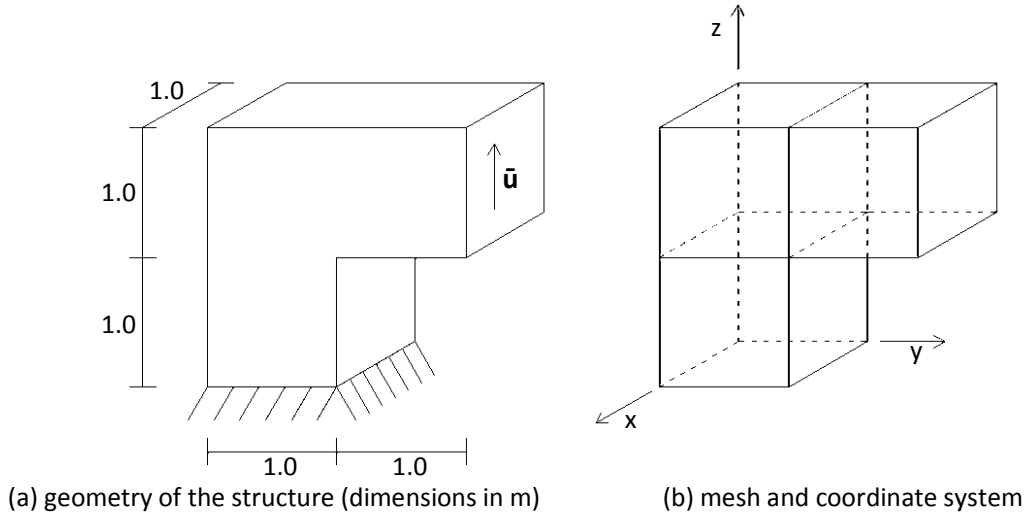


Figure 1 – L-shaped structure with full moment connection and imposed displacement at the tip

Figure 2 and 3 clearly display the three-dimensional damaged solid, whereas Figures 4, 5 and 6 present some of the stress fields in the structure's bisector plane, which is defined by $x = 0.5$ m. The geometry of the structure and the load make the presented stresses more significant than the others because the solid's behaviour has parallel with a plate.

Figure 2 and 3 illustrate the evolution of damage, which, as expected, starts in the area with greater stresses. Inward corners are likely to accumulate higher and more acute stresses and this formulation appears to be able to model that concentration. The three-dimensional effect is obvious in Figure 2 (b) and Figure 3 (b), since damage appears in the interior of the structure, where σ_{xx} is more relevant. Moreover, damage also appears in the fixed support, where tensile stresses are bound to appear. In this point, damage models give distinct results, since Comi and Perego's model concentrates damage in the inward corner, while Mazars model spreads damage from this point to the fixed support. It is important to bear in mind that the nonlocal variables are different in each model, the elastic energy release rate, Y , and the equivalent strain, $\bar{\epsilon}$, respectively.

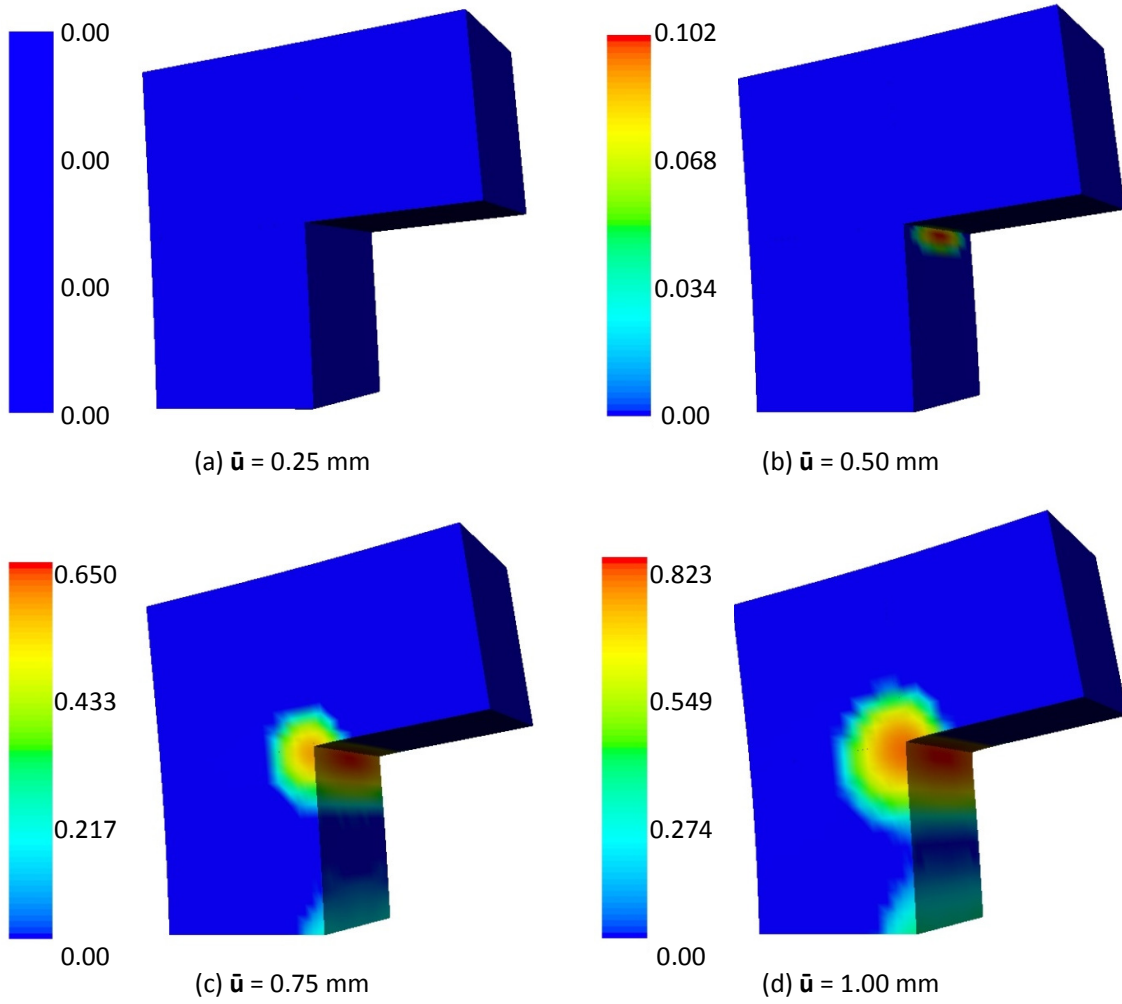
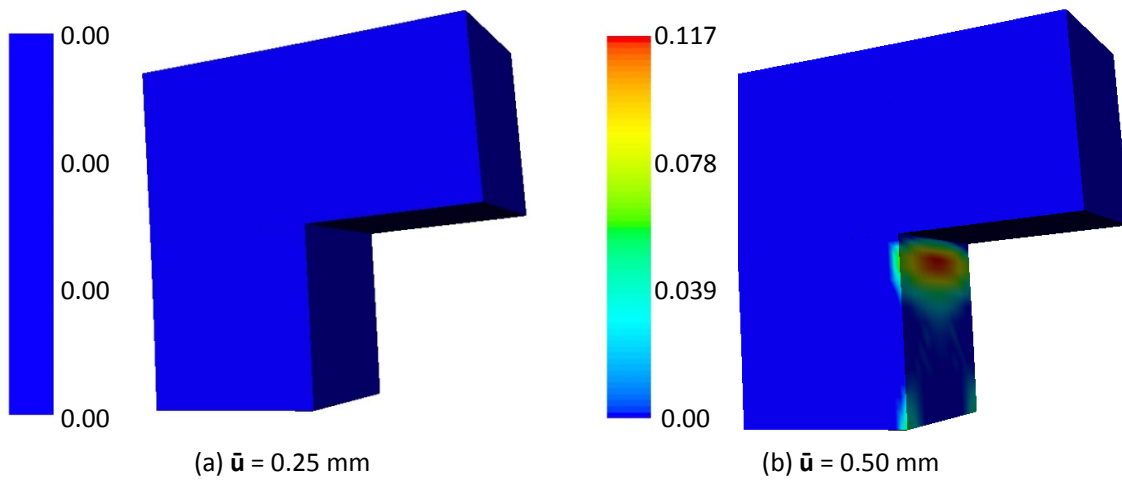


Figure 2 – Evolution of damage following Comi and Perego's model in the L-shaped structure (deformed configuration with a scale factor of 100)



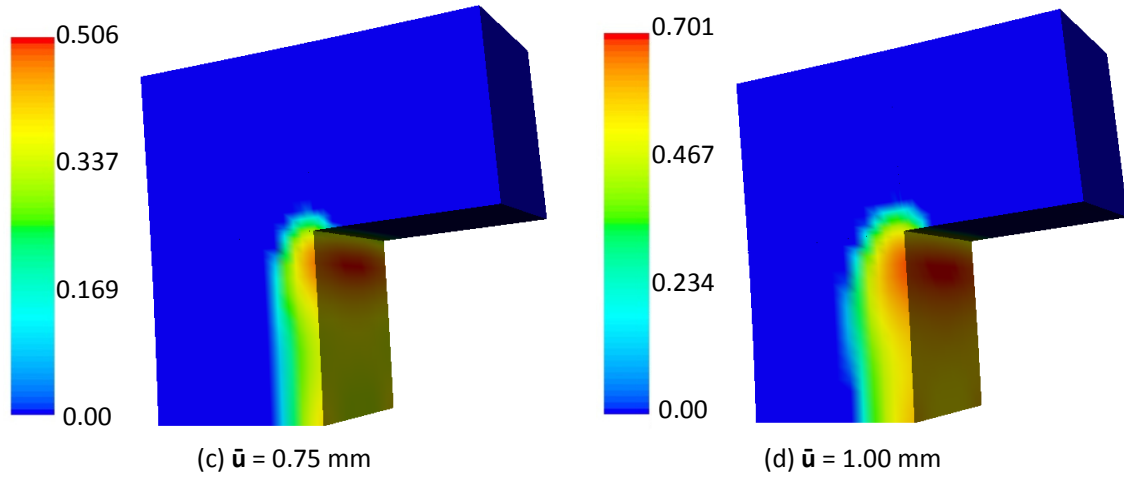


Figure 3 – Evolution of damage following Mazars model in the L-shaped structure (deformed configuration with a scale factor of 100)

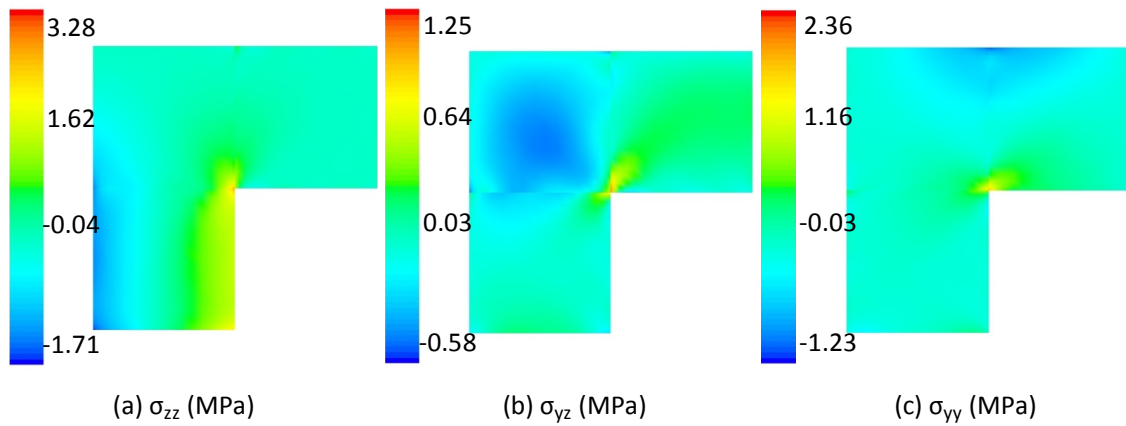


Figure 4 – Elastic stress diagrams in the L-shaped structure ($\bar{u} = 0.25$ mm)

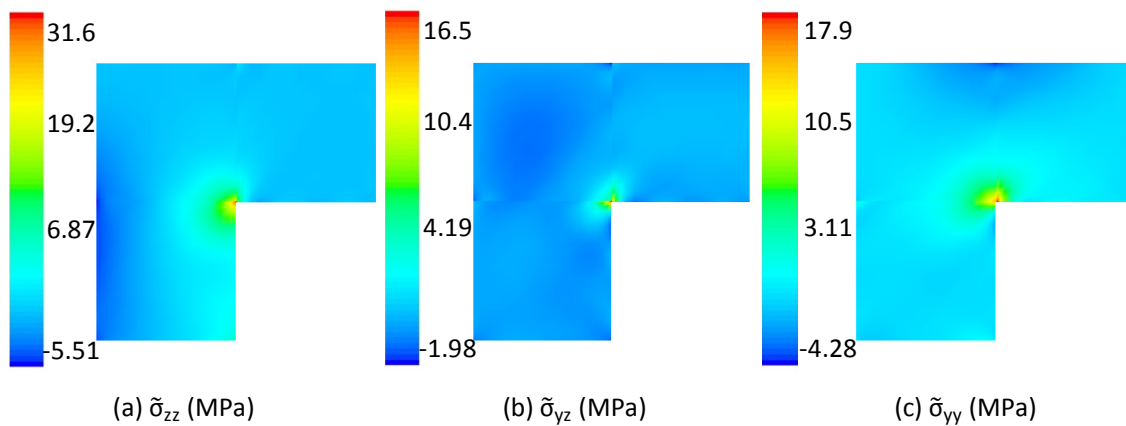


Figure 5 – Effective stress fields in the L-shaped structure in nonlinear analysis ($\bar{u} = 1.00$ mm) following Comi and Perego's damage model

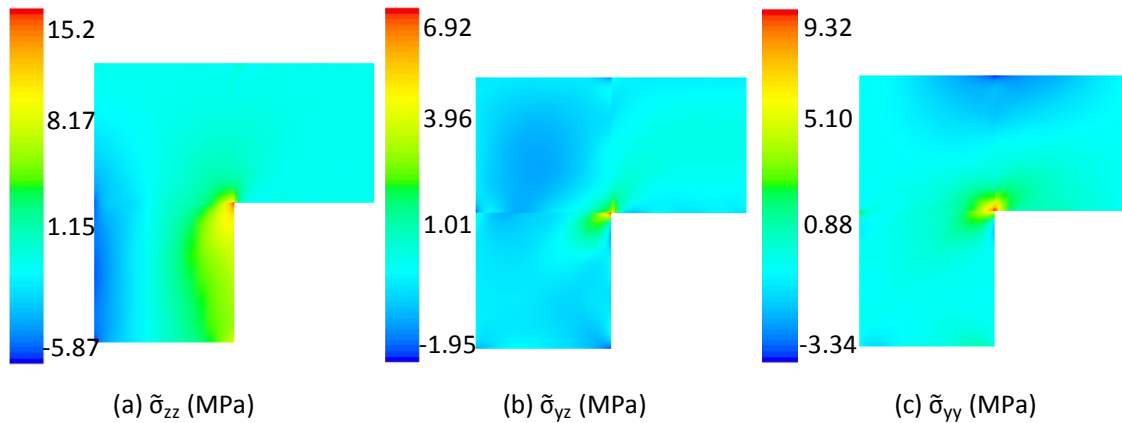


Figure 6 – Effective stress fields in the L-shaped structure in nonlinear analysis ($\bar{u} = 1.00$ mm) following Mazars damage model

These responses are clearly an approximation of reality, which seem to give kinematically admissible solutions, but fail to give a statically admissible solution. The deformed configurations of the structure and the effective stress fields attest these conclusions. On the one hand, the deformed configuration depicted in Figures 2 and 3 induces that the result is kinematically admissible as the boundaries of adjoining finite elements are still coincident, even though there is in fact a discrepancy between boundary displacements, which is only perceptible with lower degrees of approximation and zooming in. On the other hand, the discrepancy between stress fields is notorious, which are depicted in Figures 4, 5 and 6. The conventional ways of improving a solution in basic finite element methodology, either applying h-refinements or p-refinements, should be applied to have a better compliance of the stress fields.

6.2. Analysis of a fixed-fixed beam

The next example shows a beam under a distributed load and compares these results to those of the same beam considering only its self-weight, γ . The most relevant data is given in Figure 7. The structure was modelled taking $n_v = 6$ and $n_g = 5$.

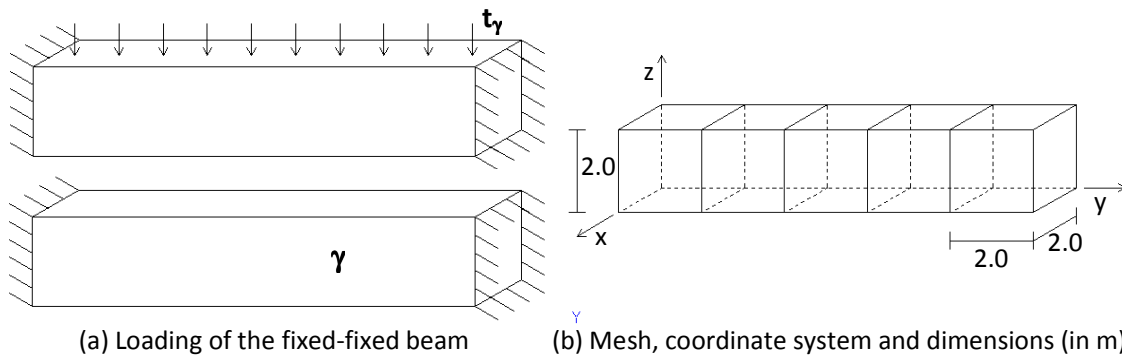
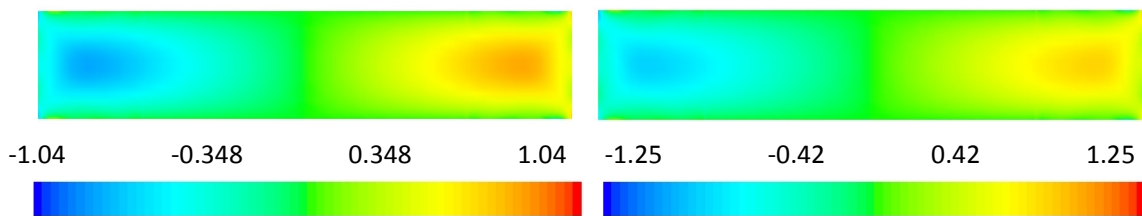


Figure 7 – The fixed-fixed beam

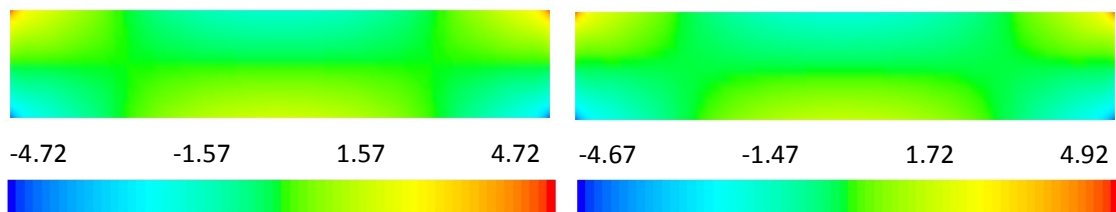
Actually, the cross section is too thick to consider that the structure is a beam, but only in such a case is it worthy to use three-dimensional elements in the modelling process. Furthermore, in this example it is possible to qualitatively relate the given stresses to the well-known internal loads expected to occur in a beam. For instance, it is known that in this structure the highest bending moments are in the supports and, hence, this is where the highest stress values occur. Moreover, the shear stresses of a rectangular section in elastic regime is known to assume a parabolic distribution and, in a structure such as this, to have maximum values at the supports. This is coherent with Figure 8, disregarding the perturbations close to the fixed end. Bending moments are negative at the supports and positive at mid-spam, thus, tensile stresses occur at the top fibers of the fixed ends and bottom fibers of mid-spam, as Figure 9 shows. Finally, damage begins and evolves in the fixed ends of the beam, as Figure 10 attests. In case of a ductile material, this is where the plastic hinges would, in fact, first appear.



(a) $\gamma = 125 \text{ kN/m}^3$

(b) $t_\gamma = 250 \text{ kN/m}^2$

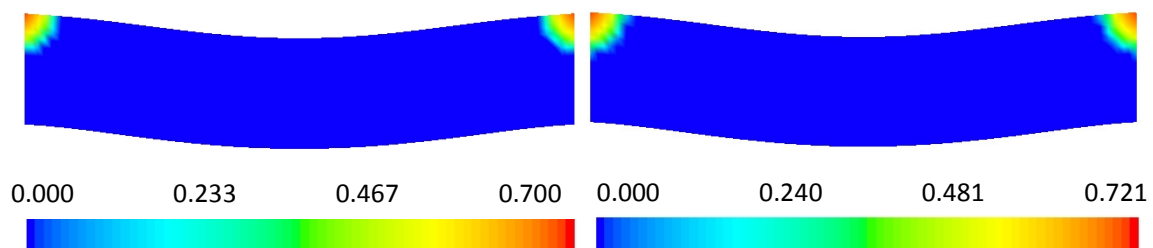
Figure 8 – σ_{yz} (MPa) stresses of the fixed-fixed beam in elastic regime



(a) $\gamma = 125 \text{ kN/m}^3$

(b) $t_\gamma = 250 \text{ kN/m}^2$

Figure 9 – σ_{yy} (MPa) stresses of the fixed-fixed beam in elastic regime



(a) $\gamma = 125 \text{ kN/m}^3$

(b) $t_\gamma = 250 \text{ kN/m}^2$

Figure 10 – Damaged beam following Comi and Perego's damage model (deformed configuration with a scale factor of 500)

7. Conclusions and further developments

On the one hand, it is now possible to model different structures in elastic regime more efficiently using the presented analytical expression for the integration of the product of the derivatives of Legendre polynomials. On the other hand, continuum damage mechanics provides a robust framework to model the nonlinear behaviour of materials, namely concrete. Besides, its versatility allows the derivation of different damage models, which plays an important role in this thesis since two models are applied and, thus, the coherence between their results underlines that the implementations are fit to analyse three-dimensional structures considering their physically nonlinear behaviour.

Accepting the limitations regarding the fact that the model focuses on providing solutions respecting the kinematic conditions and considering the fairly sound results presented in section 6, the key-conclusion of this work is that hybrid displacement models provide reliable results. However, some drawbacks are not easy to cap. For instance, the lack of intuitiveness associated with the models is not appealing. However, the greatest problem is undoubtedly the computational cost of the model. In fact, the three-dimensional simulation of a complex structure is far from being attainable in a short period of time if damage occurs.

Further developments concern both overcoming presented limitations and extending the application field of this formulation. Among others:

1. Parallel processing would decrease the simulation time considerably.
2. Limiting the considered neighbourhood of each point when applying the regularization method decreases the simulation time, even though conceptually it is not as correct as the implemented version. Nevertheless, in practical terms the results might be nearly the same.
3. The applied convergence method is a secant method. It might be useful to compare its performance with others which take less iterations to reach convergence. In fact, the secant method would be more adequate if computing the governing system was not as time-consuming as it is even in simple examples as the presented in this paper.
4. The developed program should be able to model finite elements with geometrical shapes other than rectangular prisms, namely, any kind of cuboids and solids with curve faces. The first case is rather easy, since the only additional difficulty is that the Jacobian of the coordinate transformation from the parent element to the global coordinate system is not constant. Elements with curved faces require not only what is mentioned above, but also a greater number of nodes to detail the structure.
5. The development and optimization of an implementation which introduces damage as a corrective term on the right-hand-side of the governing system might be profitable. Besides, the improvement of an iterative process of solving the governing system with the conjugate

- gradient method might allow the use of h-refinements and p-refinements in the studied structures without unreasonable computational memory costs.
6. The introduction of different damage models may yield more accurate results, namely if the models consider irreversible strains and unloading is foreseen.
 7. The most demanding development is probably to implement a unified framework for continuum damage and fracture mechanics, able to model the initial diffuse microcracking of concrete and the coalescent macrocracks that appear as damage develops.

8. Acknowledgements

I want to thank Fundação para a Ciência e Tecnologia (PTDC/ECM/71519/2006) for the financial support, which is, in fact, a great incitement to give the first steps in the demanding work of scientific investigation, and I thank Professor Luís Castro for helping and accompanying me in these steps.

9. References

- Bascoul, A. (1996). State of the art report - Part 2: Mechanical micro-cracking of concrete. *Matériaux et Constructions/Materials and Structures* , 29, 66-78.
- Bažant, Z. P. (1984). Imbricate continuum and progressive fracturing of concrete and geomaterials. *Meccanica* , 14, 86-93.
- Bažant, Z. P. and Pijaudier-Cabot, G. (1988). Nonlocal continuum damage, localization instability and convergence. *Journal of Applied Mechanics* , 55 (June), 287-293.
- Beyer, W. H. (1987). *CRC Standard Mathematical Tables*. CRC Press, Boca Raton.
- Borino, G. and De Borst, R. (2000). Some observations on the regularizing field for gradient damage models. *Acta Mechanica* , 140, 149-162.
- Comi, C. and Perego, U. (2001). Nonlocal aspects of nonlocal damage analyses of concrete structures. *European Journal of Finite Elements* , 10, 227–242.
- Comi, C., Mariani, S. and Perego, U. (2002). On the transition from continuum nonlocal damage to quasi-brittle discrete crack models. *Third Joint Conference of Italian Group of Computational Mechanics and Ibero-Latin American Association of Computational Methods in Engineering* .
- Freitas, J. A., Almeida, J. P. and Pereira, E. M. (1999). Non-conventional formulations for the finite element method. *Computational Mechanics* , 23, 488-501.
- Lemaitre, J. and Desmorat, R. (2005). *Engineering Damage Mechanics*. Springer Berlin Heidelberg.

Lemaitre, J., Benallal, A., Billardon, R. and Marquis, D. (2002). Thermodynamics and phenomenology. In *Continuum Thermomechanics - The Art and Science of Modelling Material Behaviour, Solid Mechanics and Its Applications* (Vol. 76, pp. 209-223). Springer Netherlands.

Lopes, M. et al (2008). *Sismos e Edifícios*. Edições Orion.

Mazars, J. (1984). *Application de la mécanique de l'engoulement au comportement non linéaire et à la rupture du béton de structure - Doctoral Programme Thesis*. Paris: Université Paris 6.

Mazars, J., Pijaudier-Cabot, G. and Saourdis, C. (1991). Size effect and continuous damage in cementitious materials. *International Journal of Fracture* , 51, 159-173.

Perego, M. (1990). *Danneggiamento dei materiali lapidei: leggi costitutive, analisi per elementi finiti ed applicazioni - Doctoral Programme Thesis*. Politecnico de Milano.

Pereira, E. M. and Freitas, J. A. (2000). Numerical Implementation of a Hybrid-Mixed Finite Element Model for Reissner-Mindlin Plates. *Computers & Structures* , 74, 323-334.

Silva, M. C. (2006). *Modelos de Dano em Elementos Finitos Híbridos e Mistos, Dissertação para obtenção do grau de Doutor em Engenharia Civil*. Instituto Superior Técnico - Universidade Técnica de Lisboa.

Zienkiewicz, O. C. (1977). *The Finite Element Method* (3rd edition ed.). McGraw-Hill.